

## Controlling the degree of visibility of Young's fringes with photon coincidence measurements

P. H. S. Ribeiro, S. Pádua, J. C. Machado da Silva, and G. A. Barbosa\*

*Departamento de Física, Instituto de Ciências Exatas, Universidade Federal de Minas Gerais, Caixa Postal 702, CEP 30161-970, Belo Horizonte, Minas Gerais, Brazil*

(Received 6 December 1993)

Is it possible to detect the interference from an extended incoherent source with Young's slits when the source-slits distance is such that all dimensions of the coherence area of the incident light beam are smaller than the distance between the slits? We have experimentally demonstrated that, under the above conditions, interference fringes can be obtained with a controlled degree of visibility by means of coincidence measurements between conjugated beams of the down-conversion luminescence.

PACS number(s): 42.50.-p

### I. INTRODUCTION

It is a known fact that the Young's double-slit experiment, done with an extended incoherent quasi-monochromatic light source, generates an interference pattern when one dimension of the coherence area, the dimension corresponding to the direction of the ray vector joining the slits, is larger than the separation between slits. This subject has been discussed in great detail by Born and Wolf [1] in their presentation of the Van Cittert-Zernike theorem. Coherence area measurements are often used in applications where light is produced by an extended source. From the knowledge of this area, we can estimate the size of the source needed in interference and diffraction experiments [1].

The use of parametric down-conversion as a source of photon pairs has had a great interest in quantum optics experiments as it is shown by the large number of articles published in the subject in the last eight years [2,3]. In a recent experiment [4], the coherence area was measured in a Young's experiment using parametric down-conversion light generated by a nonlinear crystal. The experiment was done with only one of the beams from the parametric down-conversion and the intensity distribution of the transmitted light, measured for several source-slits distances. At the point where the interference fringes pattern disappear, one dimension of the coherence area is equal to the separation between the slits, giving the way to determine the coherence area. For even shorter source-slits distances, the interference fringes pattern disappear as expected for extended quasimonochromatic incoherent sources [1].

We report a Young's slits experiment done with down-converted light and measured with *coincidence* techniques. Coincidences between the transmitted light beam (signal) through the Young's slits and its conjugated

beam (idler) are measured. A completely different result is found for this second-order coherence experiment when compared with the results [4] for the first-order ones. Of course, we cannot expect those results to be the same because correlation functions of different order are involved. However, some physical insight can be gained through this simple comparison. Fringes interference patterns are detected for several source to slit distances, even for distances as short as 20 mm which was the minimum possible distance for the setup. On the other hand, for a fixed distance between the source and idler beam detector, it is observed that the interference pattern is dependent on the idler pinhole diameter in front of the detector.

These results appearing in coincidence measurements between the down-converted beams, indicate that the classical Van Cittert-Zernike theorem could be extended to second-order experiments including the nonlocal dependence between signal and idler beams.

### II. EXPERIMENTAL SETUP

Most of our experimental setup has been described in previous work [4]. Parametric down-conversion luminescence is produced by a  $\text{LiIO}_3$  nonlinear crystal when it is pumped by a 100 mW argon-ion laser emitting at 3511 Å. Two beams with wavelengths around 7887 Å (signal) and 6328 Å (idler) are chosen by setting the detectors at angles  $32^\circ$  (signal) and  $25^\circ$  (idler) with respect to the pump beam direction and by using filters with bandwidth 400 Å and 100 Å respectively, at the photomultiplier tube entrances. Pinholes mounted in two-dimensional stages (Fig. 1) are used for defining the signal and idler beams directions [ $\phi(P_1) = 0.6$  mm,  $\phi(P_2) = 2.0$  mm, and  $\phi(P_3) = 0.5$  mm]. The nonlinear crystal is mounted in a rotating stage to enable us to fine tune the phase-matching angle. The crystal used is 20 mm long, and the laser beam, measured by scanning it spatially with a small pinhole coupled to a power meter, is Gaussian with

---

\*Electronic address: gbarbosa@fisica.ufmg.br

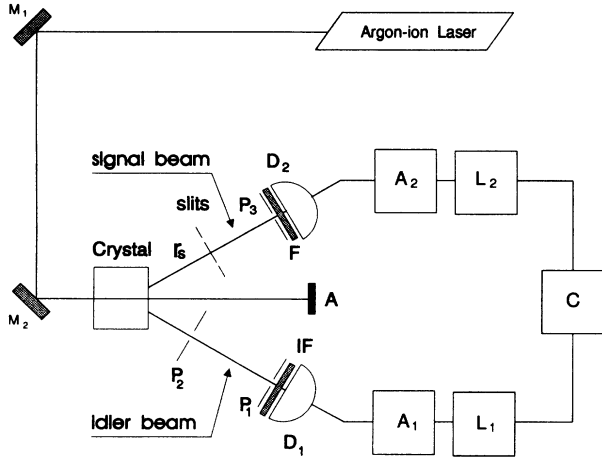


FIG. 1. Schematic diagram of the experimental setup for Young's double-slit experiment.  $M_1$  and  $M_2$  are mirrors;  $P_1$ ,  $P_2$ , and  $P_3$  are pinholes;  $D_1$  and  $D_2$  are photomultipliers; IF is an interference filter;  $F$  is an absorption filter;  $A$  is a beam stop;  $A_1$  and  $A_2$  are pulse formatting devices;  $L_1$  and  $L_2$  are delay lines;  $C$  is the coincidence detection system; and  $r_s$  is the distance between source and slits.

a 1.0 mm full width at half maximum (FWHM).

The Young's slits are made by a photographic process, producing a dark negative with two transparent slits. The width of each slit and the distance between them, measured with a microscope, are  $80 \mu\text{m}$  and  $90 \mu\text{m}$ , respectively. The slits are aligned along the plane of the pump laser and the down-converted beams. Interference fringes are detected by means of coincidence measurements between the idler beam and the transmitted signal beam through the Young's slits. The detector at the idler beam is kept fixed while the signal beam detector is scanned in the direction perpendicular to the larger slits dimension.

The detectors are photomultipliers (PMT) cooled by water and a Peltier cooling system. Pulses from the photomultipliers are amplified, discriminated, and formatted before they are sent to the counters. All data is transferred and processed by an IBM compatible personal computer. A multichannel analyzer is also used to obtain a histogram of the time delay between photons.

### III. RESULTS

A theory to fit the experimental points obtained is not yet available. However, the fact that the shape of the coincidence patterns (Fig. 2) is quite similar to the ones obtained in a first-order coherence experiment, suggests that we define a phenomenological function to fit the experimental points, and present a physical justification for it along the paper. The function is

$$E(Q) = E_0(Q)[1 + \mu_E \cos(\alpha_E + \delta)], \quad (1)$$

where  $E(Q)$  is the *coincidence excess* with the signal beam detector at the point ( $Q$ ),  $\mu_E$  is an adjustable pa-

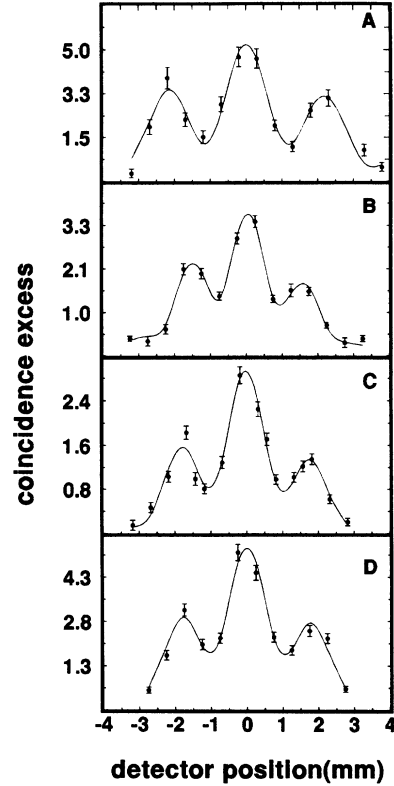


FIG. 2. Experimental points showing the coincidence excess as a function of the detector position and fittings. The distance between source and slits and visibilities are in (a),  $r_s = 295 \text{ mm}$  and  $\mu_{12} = 0.57 \pm 0.06$ ; in (b),  $r_s = 80 \text{ mm}$  and  $\mu_{12} = 0.44 \pm 0.03$ ; in (c),  $r_s = 35 \text{ mm}$  and  $\mu_{12} = 0.52 \pm 0.05$ ; in (d),  $r_s = 20 \text{ mm}$  and  $\mu_{12} = 0.46 \pm 0.06$ . The pinhole  $P_1$  diameter is  $\phi(P_1) = 0.6 \text{ mm}$ .

rameter,  $\delta$  is the path difference between fields originating at slit 1 and slit 2,  $\alpha_E$  is also adjustable and  $E_0(Q)$  is given by

$$E_0(Q) = E_{0N} \left( \frac{\sin k_s x}{k_s x} \right)^2, \quad (2)$$

where  $E_{0N}$  is a normalization factor, and  $x$  is the variable coordinate of the point ( $Q$ ).

The above mentioned *coincidence excess* is defined by

$$E = \frac{C - C_A}{C_A}, \quad (3)$$

where  $C$  is the coincidence rate,  $C_A = C_1 C_2 \tau_R$  is the accidental coincidence rate,  $C_1$  is the PMT<sub>1</sub> counting rate,  $C_2$  is the PMT<sub>2</sub> counting rate, and  $\tau_R$  is the resolution time for the coincidences.

The coincidence patterns for four distances between source and slits and fittings are shown in Fig. 2. They were obtained with a sampling time of 1800 s in each point and a resolution time of 10 ns for the coincidences.

For the closest source to slit distance, coincidence interference patterns were obtained with the diameter of the pinhole  $P_1$  increased from  $\phi(P_1) = 0.6 \text{ mm}$  to  $\phi(P_1) =$

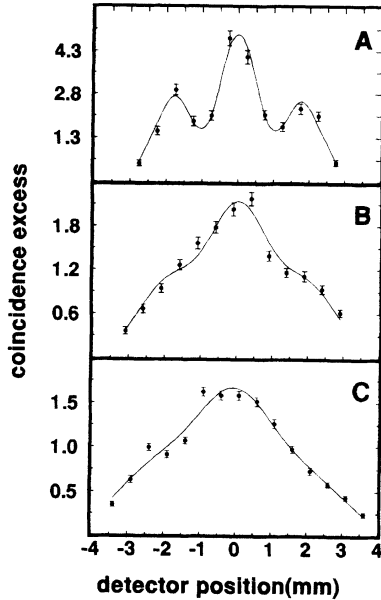


FIG. 3. Coincidence interference patterns for different diameters of pinhole  $P_1$ . Source to slits distance is  $r_s = 20$  mm. The pinhole  $P_1$  diameters and visibilities are  $\phi(P_1) = 0.6$  mm and  $\mu_{12} = 0.46 \pm 0.06$  in (a),  $\phi(P_1) = 1.8$  mm and  $\mu_{12} = 0.13 \pm 0.04$  in (b), and  $\phi(P_1) = 3.0$  mm and  $\mu_{12} = 0.09 \pm 0.04$  in (c).

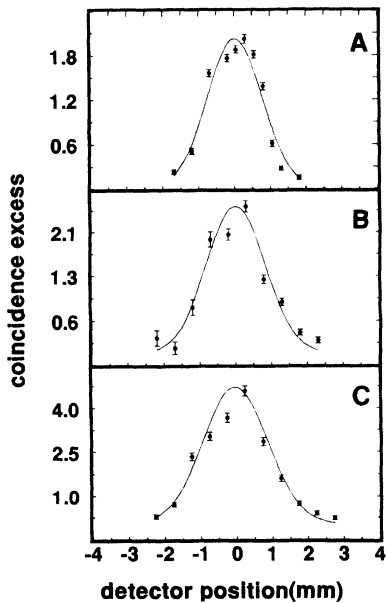


FIG. 4. Coincidence source profiles and fittings. The  $P_1$  diameter is  $\phi(P_1) = 0.6$  mm. The distances  $r_d$  between source and signal beam detector and the Gaussians FWHM are  $r_d = 130$  mm and  $\sigma = 1.82 \pm 0.16$  mm in (a),  $r_d = 250$  mm and  $\sigma = 1.92 \pm 0.18$  mm in (b), and  $r_d = 430$  mm and  $\sigma = 2.13 \pm 0.15$  mm in (c). The projected width on the source position is  $\sigma_0 = 1.67 \pm 0.23$  mm.

1.8 mm and to  $\phi(P_1) = 3.0$  mm. The patterns and fittings are shown in Fig. 3.

Coincidence source profiles were obtained by making the same kind of measurements without slits. For the pinhole  $P_1$  with diameter  $\phi(P_1) = 0.6$  mm, these profiles are shown in Fig. 4 for three distances  $r_d$  between source and detector. The sampling time was reduced to 300 s, because of the signal increase without slits. Fitting these profiles with a Gaussian function we can obtain information about the effective size of the source for coincidence experiments.

#### IV. DISCUSSION

The function chosen to fit the experimental points is analogous to the expression for the intensity interference patterns in first-order coherence experiments. This analogy can lead us to interesting conclusions about the measurements.

The parameter  $\mu_E$  in expression (1) is the counterpart of the Young's fringes visibility in a first-order coherence experiment. We compare in Table I the *coincidence visibility*  $\mu_E$  obtained by the fittings, with the prediction for the visibility  $\mu_{12}$  in a first-order coherence experiment [1,4] with the same parameters of the second-order coherence experiment performed. While the fittings are rather good, the *coincidence visibility*  $\mu_E$  is always larger than the first-order prediction of  $\mu_{12}$ , even for short distances between source and slits. Note that those values for  $\mu_E$  cannot be explained even by a small effective source size measured with coincidence detection, since the measured size,  $\sigma_0 = 1.67 \pm 0.23$  mm, is not small (see Fig. 4).

It is clearly shown that it is not possible to use the first-order coherence theory to fit the second-order coherence experiment results, even noting that the patterns produced by the two kinds of experiments are very alike. However, the profiles shown in Fig. 3, in which the *coincidence visibility*  $\mu_E$  is decreased by increasing the idler beam pinhole ( $P_1$ ) diameter, indicate how to use the first-order coherence theory to understand qualitatively the behavior of the coincidence patterns.

An extended incoherent source, produces a superposition of interference patterns after the Young slits, due to each light mode present in the radiation field. The frequency range is determined by a narrow width filter ( $\sim 100$  Å) in the idler beam and a certain range of wave vectors  $\vec{k}_s$  is accepted through the slits. As the detec-

TABLE I. Comparison between the degree of visibility  $\mu_{12}$  given by a first-order coherence theory and the experimentally obtained  $\mu_E$  through coincidence measurements.

Source-slits distance (mm)	Visibilities	
	$\mu_E$	$\mu_{12}$
295	$0.57 \pm 0.06$	0.23
80	$0.44 \pm 0.03$	$\sim 0$
35	$0.52 \pm 0.05$	$\sim 0$
20	$0.46 \pm 0.06$	$\sim 0$

tion of the interference patterns is done by a coincidence scheme, only photons which have a twin on the conjugated beam will be detected within the photons of the superposed patterns.

When we vary the idler beam detector pinhole ( $P_1$ ) diameter as in Fig. 3, we are selecting idler beam wave vectors  $\vec{k}_i$ . As the momentum conservation implies in a strong correlation between the twin photons wave vectors, the signal beam wave vectors  $\vec{k}_s$  are also selected within the collected signal light by the coincidence detection. In other terms, only some interference patterns are selected, resulting in the control of the fringes visibility by means of the idler beam pinhole diameter ( $P_1$ ). In this way, interference can always be detected, even if the slits are very close to the source.

Of course a second-order coherence theory must be developed to *quantitatively* show the complete dependence of the coincidence patterns on the system parameters, but this qualitative explanation based on first-order coherence concepts is useful to the understanding of this interesting selection mechanism. This mechanism explaining the *selection* of first-order patterns within the superposed patterns, justifies the form adopted for the coincidence excess given by Eq. (1).

## V. CONCLUSIONS

The Young's double-slit experiment was performed using the signal beam of the parametric down-converted light and coincidence measurements were made between these photons and the conjugated idler photons.

These measurements show interference fringes with a reasonable contrast, even when the light transmitted through the slits is incoherent in the sense that all dimensions of the first-order coherence area are smaller than the distance between slits. This is possible if we use the coincidence detection scheme with the beam without slits being detected under conditions that permit the selection of the *coherent photons*. We also demonstrated that the degree of Young's fringe visibility can be controlled through the conjugated idler beam.

Analogously as done in the classical Van Cittert-Zernike theorem for the first-order correlation function that gives the coherence area for the electric field, the results shown in this work suggest that *entangled coherence areas* could be *simultaneously* specified for the conjugated *signal* and *idler* beams through the second-order correlation function.

## ACKNOWLEDGMENTS

This work was supported by FINEP (Financiadora de Estudos e Projetos) and CNPq (Conselho Nacional de Desenvolvimento Científico e Tecnológico), Brazil. We are indebted to Professor A. L. de Oliveira and Professor A. S. Chaves from Universidade Federal de Minas Gerais, Brazil, for lending us some equipment and specially to Professor Jacques Bouillot from Faculté Annécienne des Sciences et Techniques, France, for supplying the excellent quality  $\text{LiIO}_3$  crystal. We also thank Dr. C. H. Monken for helpful hints concerning the coincidence system and Dr. Patrice Bourson for information about nonlinear crystals.

- 
- [1] M. Born and E. Wolf, *Principles of Optics*, 2nd ed. (Pergamon Press, New York, 1964), pp. 499–513.  
 [2] D. Greenberger, M. A. Horne, and A. Zeilinger, *Phys. Today* **49**, 22 (1993).

- [3] L. Wang, Ph.D. thesis, University of Rochester, 1992 (unpublished).  
 [4] P. H. S. Ribeiro, C. H. Monken, and G. A. Barbosa, *Appl. Opt.* **33**, 352 (1994).

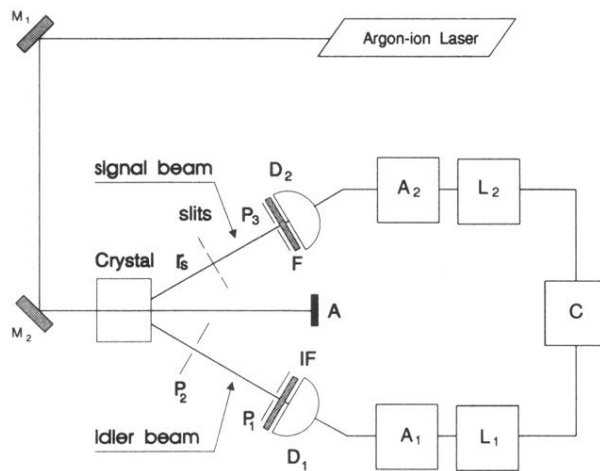


FIG. 1. Schematic diagram of the experimental setup for Young's double-slit experiment.  $M_1$  and  $M_2$  are mirrors;  $P_1$ ,  $P_2$ , and  $P_3$  are pinholes;  $D_1$  and  $D_2$  are photomultipliers; IF is an interference filter;  $F$  is an absorption filter;  $A$  is a beam stop;  $A_1$  and  $A_2$  are pulse formatting devices;  $L_1$  and  $L_2$  are delay lines;  $C$  is the coincidence detection system; and  $r_s$  is the distance between source and slits.